Antimony Complexes

Deutsche Ausgabe: DOI: 10.1002/ange.201503074
Internationale Ausgabe: DOI: 10.1002/anie.201503074

Reductive Catenation of Phosphine Antimony Complexes**

Saurabh S. Chitnis, Neil Burford, Jan J. Weigand,* and Robert McDonald*

Abstract: *Reactions of triarylphosphines with fluoroantimony(III) triflates give phosphine antimony(III) complexes, which undergo spontaneous reductive elimination of fluorophosphonium cations. The resulting phosphine antimony(I) complexes catenate to give the first examples of cationic antimony bicyclic compounds, $[(R_3P)_4Sb_6]^{4+}$, featuring a bicyclo[3.1.0]hexastibine framework stabilized by four phosphine ligands. The unprecedented 14-electron redox process illustrates the generality of the reductive catenation method.*

Homoatomic monocyclic (**A**), bicyclic (**B**), and cage (**C**) frameworks are fundamental molecular structures, exhibited typically by boron, carbon, silicon, sulfur, and phosphorus. Although examples of anionic ($k<0$) or neutral ($k=0$) frameworks are known for most metalloids,[1] cationic monocycles (**A**, $k>0$) and bicycles (**B**, $k>0$) derived from metalloids are rare and are limited to selenium, tellurium, silicon, and germanium.[2] The remarkable electronic properties measured for *catena*-silicon systems[3] have the potential to be exhibited by other metalloids, but their discovery is precluded by the absence of synthetic routes to catenated molecular frameworks.

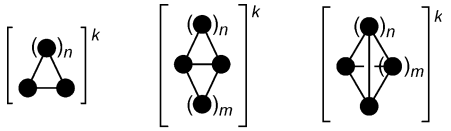

We have developed a versatile reductive catenation method that involves the use of phosphines (or arsines) as both ligands and reductants.[4] Complexes of antimony or phosphorus acceptors have been demonstrated to undergo 2-electron,[4a] 8-electron,[4b,c] 10-electron,[4d] or 18-electron[4e] redox processes to give the *catena*-pnictogen cations, $[\mathbf{1}]^{2+}$, $[\mathbf{2}]^{4+}$, $[\mathbf{3}]^{2+}$ and $[\mathbf{5}]^{3+}$, respectively (Figure 1). We now report an unprecedented 14-electron reductive catenation to form the cation $[(Ph_3P)_4Sb_6]^{4+}$, denoted $[\mathbf{4}]^{4+}$, which is the first example of framework **B** ($k>0$) for antimony.

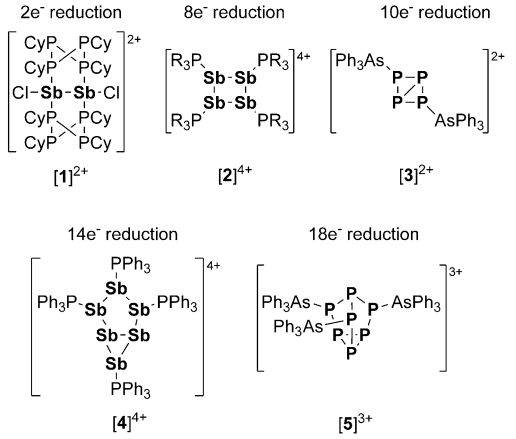

Figure 1. *Catena*-pnictogen cations accessible by reductive catenation.

The reaction of $FSb(OTf)_2$ with two equivalents of PPh_3 in MeCN yields $[(Ph_3P)_2SbF(OTf)_2]$, denoted $\mathbf{6}(OTf)_2$, which has been isolated and comprehensively characterized. In the solid state, the antimony center in $\mathbf{6}(OTf)_2$ adopts a square-based pyramidal geometry consistent with one stereochemically active lone pair located *trans* to the apical fluorine substituent (Figure 2). The phosphine ligands are *trans* configured with respect to each other as are the triflate substituents. The P–Sb distances (2.8304(6), 2.7870(6) Å) are similar to those in $[(Ph_3P)_2SbCl_3]$ (2.7934(4) Å)[5] and, together with the short Sb–O distances (2.2426(18) and 2.23(3) Å, compared to the sums of the Sb and O van der Waal's radii, $\Sigma_{r,vdW}=3.60$ Å,[11a] and the covalent radii, $\Sigma_{r,cov}=2.05$ Å[11b]), are consistent with a molecular rather than ionic formulation for $\mathbf{6}(OTf)_2$ in the solid state.

Yellow solutions of $\mathbf{6}(OTf)_2$ in MeCN exhibit a signal in the ^{31}P NMR spectrum at $\delta_P=16.0$ ppm (compared with -5.6 ppm for PPh_3) that is broad ($\nu_{1/2}=90$ Hz), consistent with the phosphorus centers being bound to quadrupolar antimony nuclides ($I(^{121}Sb)=5/2$, $I(^{123}Sb)=7/2$) and dynamic exchange.[13] In the ^{19}F NMR spectrum, a signal for the Sb–F moiety of $\mathbf{6}(OTf)_2$ at $\delta_F=-117.5$ ppm is significantly shielded compared to that of free $FSb(OTf)_2$ (-95.3 ppm), but deshielded compared to those for derivatives of $[(R_3P)_2SbF]^{2+}$ (R = Me, Et, Pr, Bu; range of $\delta_F=-173.4$ to -187.1 ppm),[4b] likely as a result of the relatively low basicity

[*] Dr. S. S. Chitnis, Prof. N. Burford
Department of Chemistry, University of Victoria
P.O Box 3065, Stn. CSC, Victoria (Canada)
E-mail: nburford@uvic.ca
Prof. J. J. Weigand
Fakultät Chemie und Lebenschmittelchemie
Technische Universität Dresden
01062 Dresden (Germany)
E-mail: jan.weigand@tudresden.de
Dr. R. McDonald
Department of Chemistry, University of Alberta
1227 Saskatchewan Dr. NW, Edmonton (Canada)

[**] We thank the Natural Sciences and Engineering Research Council of Canada and Vanier Canada Graduate Scholarships Program (S.S.C.) for funding. We gratefully acknowledge financial support from the ERC (SynPhos 307616) for a six-month research stipend for S.S.C. at the TU Dresden.

Supporting information for this article is available on the WWW under http://dx.doi.org/10.1002/anie.201503074.

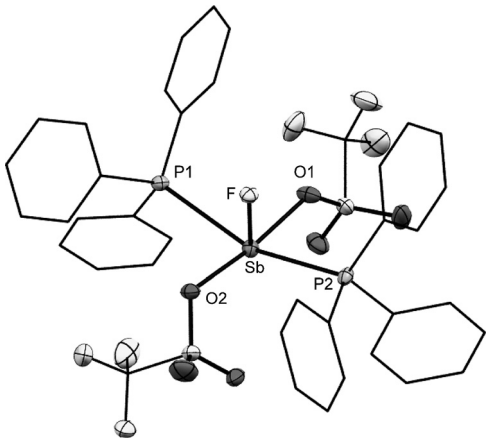

Figure 2. Molecular structure of **6**$(OTf)_2$ in the solid state. Hydrogen atoms and a slight disordering of the triflate group containing O1 have been omitted for clarity. Thermal ellipsoids are set at 30% probability. Key bond lengths [Å] and angles [°]: Sb–F 1.9126(14), Sb–P1 2.8304(6), Sb–P2 2.7870(6), Sb–O1 2.2426(18), Sb–O2 2.23(3); F-Sb-P1 77.24(4), F-Sb-P2 78.44(4), F-Sb-O1 81.37(6), F-Sb-O2 83.7(6), O1-Sb-O2 165.0(6), P1-Sb-P2 155.36(2), P1-Sb-O1 94.70(2), P2-Sb-O2 93.3(8), O2-Sb-P1 80.2(7), O1-Sb-P2 94.70(5).

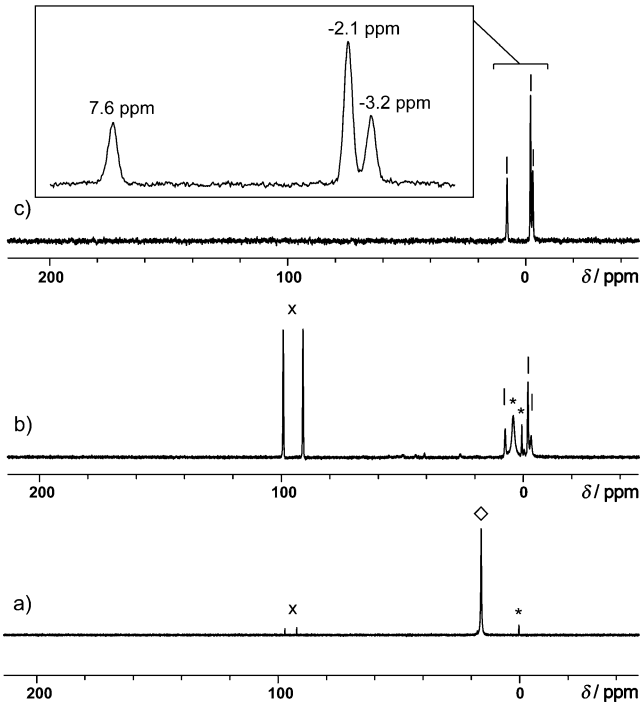

Figure 3. $^{31}P\{^1H\}$ NMR spectra (CD_3CN, 298 K) of the 1:2 reaction mixture of $FSb(OTf)_2$ and PPh_3 a) upon mixing at RT and b) after heating to 80 °C for 90 min. c) $^{31}P\{^1H\}$ NMR spectrum of a crystalline sample of [**4**][OTf]$_4$ after redissolution in CD_3CN. Symbols denote assignments for [**6**]$^{2+}$ (◇), $[Ph_3PF]^+$ (×), [**4**]$^{4+}$ (|), and unidentified products (*).

of PPh_3. The ^{19}F NMR resonance signal for the triflate substituents in **6**$(OTf)_2$ ($\delta_F = -78.8$ ppm) is comparable to that of $[PPh_4][OTf]$ (−79.4 ppm) and we therefore conclude that the triflate anions are dissociated, giving $[(Ph_3P)_2SbF]^{2+}$, denoted [**6**]$^{2+}$, in MeCN solutions of **6**$(OTf)_2$.

Within 10 minutes at ambient temperature, NMR spectra of CD_3CN solutions containing **6**$(OTf)_2$ (see Figure 3a for the $^{31}P\{^1H\}$ NMR spectrum) show new signals as a result of $[Ph_3PF]^+$ ($\delta_P = 94.7$ ppm, $\delta_F = -127.8$ ppm, $^1J_{PF} = 995$ Hz).[6] Upon heating (82 °C) for 90 min, an intensely orange-colored solution is observed. The ^{31}P NMR spectrum of this solution (Figure 3b) indicates that [**6**]$^{2+}$ has been consumed with substantial formation of $[Ph_3PF]^+$, an unassigned broad signal and three prominent broad resonances (1:2:1 intensity). The three broad resonances are assigned to [**4**][OTf]$_4$, which has been isolated (Figure 3c) and unambiguously identified by X-ray crystallography and elemental analysis. The presence of other *catena*-antimony species in the reaction mixture cannot be precluded and may be responsible for the unassigned broad resonances. Nevertheless, ^{31}P NMR spectra (Figure S1 and S2 in the Supporting Information) of reaction mixtures containing 1:1 or 1:3 mixtures of $FSb(OTf)_2$ and PPh_3 also show formation of $[Ph_3PF]^+$ and [**4**]$^{4+}$, together with residual $[(Ph_3P)SbF]^{2+}$ (1:1 stoichiometry)[12] or PPh_3 (1:3 stoichiometry). Additionally, formation of $[(p\text{-Tol})_3PF]^+$ (p-Tol = p-MePh) was detected in the 1:2 reaction mixture of $FSb(OTf)_2$ and $P(p\text{-Tol})_3$, along with a set of signals (1:2:1 intensity) assigned to a derivative of [**4**]$^{4+}$ featuring $P(p\text{-Tol})_3$ ligands (Figure S3, denoted [**4**(p-Tol)]$^{4+}$). Collectively, these observations demonstrate a thermodynamic preference for derivatives of [**4**]$^{4+}$ as the reduction product and fluorophosphonium cations as the oxidation product in the redox reaction between antimony triflates and triarylphosphines.

Separation of [**4**][OTf]$_4$ from the multiple-component reaction mixture is achieved by repeatedly washing the crude solids with MeCN to remove **6**$(OTf)_2$ and other byproducts. As a result of the multi-step workup and high sensitivity of [**4**][OTf]$_4$, the yield of the isolated product drops to 17%. The solid-state structure of [**4**][OTf]$_4$·2 MeCN·2 EtCN (Figure 4) reveals a chair conformation for the *catena*-hexastibine framework with phosphine ligands equatorially configured at four of the centers. The Sb–Sb distances in the ring (2.8200(3)–2.8642(2) Å) are shorter than those in dicationic species [**1**]$^{2+}$ (2.9150(6) Å)[4a], but comparable to those in derivatives of the tetracationic molecule [**2**]$^{4+}$ (2.8354(6)–2.884(2) Å)[4b]. Similar values are reported for neutral rings of the formula Ar_6Sb_6 (Ar = o-Tol, 2.818(1)–2.836(1) Å; Ar = m-Tol 2.828(1)–2.834(1) Å).[7] The P–Sb bond lengths in [**4**]$^{4+}$ are slightly longer (2.5875(7)–2.6377(7) Å) than in derivatives of [**2**]$^{4+}$ (2.552(2)–2.578(2) Å),[4b] likely because of the lower basicity and greater steric bulk of PPh_3. The cross-ring Sb2–Sb3-bonded distance (2.8200(3) Å) is substantially shorter than the nonbonded Sb4–Sb6 distance (4.0444(7) Å) resulting in a C_s point group for the bicyclo[3.1.0]hexastibine skeleton. Consistent with the high molecular charge, the inter-ion Sb–O contacts are in the range 2.887(6)–3.335(3) Å, significantly greater than the sum of the Sb–O covalent radii (2.05 Å).[11b]

Extrusion of $[Ph_3PF]^+$ from [**6**]$^{2+}$, is a reductive elimination and implicates formation of $[(Ph_3P)Sb]^+$ as a putative Sb^I intermediate, analogous to the formation of Fe^0 or W^{III} complexes by reductive elimination of halophosphonium cations from phosphine complexes of Fe^{II} or W^V.[8] Oligomerization of $[(Ph_3P)Sb]^+$ relieves the electron deficiency at the

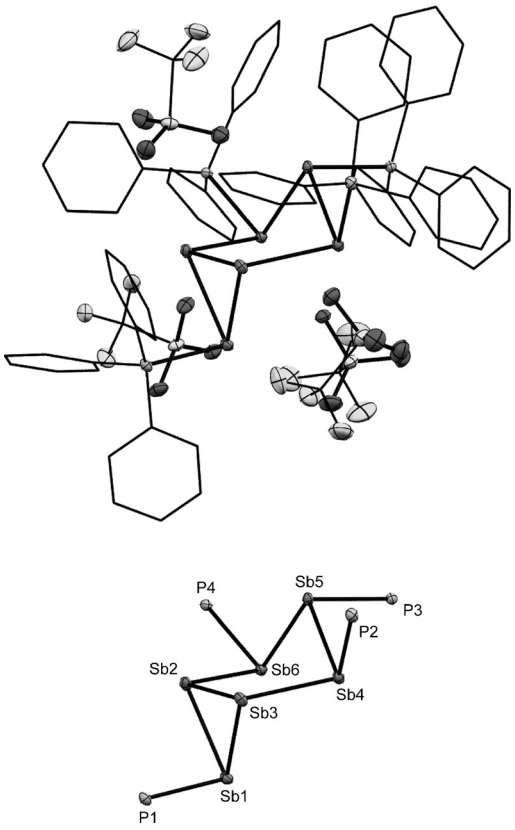

Figure 4. Top: Molecular structure of [**4**][OTf]$_4$·2 MeCN·2 EtCN in the solid state. Solvent molecules and hydrogen atoms have been omitted for clarity. Thermal ellipsoids are set at 30% probability. Bottom: Bicyclic core of the [**4**]$^{4+}$ cation with exocyclic P atoms. All other atoms have been omitted for clarity. Key bond lengths [Å] and angles [°] in [**4**]$^{4+}$: Sb1–Sb2 2.8289(3), Sb1–Sb3 2.8479(5), Sb2–Sb3 2.8200(3), Sb3–Sb4 2.8310(3), Sb4–Sb5 2.8642(2), Sb5–Sb6 2.8598(3), Sb6–Sb2 2.8443(5), Sb4–Sb6 4.0444(7), P1–Sb1 2.5875(7), P2–Sb4 2.6254(7), P3–Sb5 2.6049(7), P4–Sb6 2.6377(7); Sb1-Sb2-Sb3 60.55(1), Sb2-Sb1-Sb3 59.57(1), Sb2-Sb3-Sb1 59.88(1), Sb1-Sb2-Sb6 88.04(1), Sb2-Sb6-Sb5 9.73(2), Sb6-Sb5-Sb4 89.91(1), Sb5-Sb4-Sb3 94.08(2), Sb4-Sb3-Sb1 94.90(1), P1-Sb1-Sb2 87.25(2), P2-Sb4-Sb5 91.30(2), P2-Sb4-Sb3 91.96(2), P3-Sb5-Sb4 93.61(2), P3-Sb5-Sb6 4.97(2), P4-Sb6-Sb5 96.24(2), P4-Sb6-Sb2 91.68(2).

antimony center (6 valence electrons), as previously detected for neutral As^{I} and Sb^{I} compounds.[9] Two routes from [(Ph$_3$P)Sb]$^+$ to [**4**]$^{4+}$ are proposed in Scheme 1. Route A involves catenation of six equivalents to give the cyclo-hexa-antimony intermediate [(Ph$_3$P)$_6$Sb$_6$]$^{6+}$ (**A$_1$**, Scheme 1), whose significant molecular charge prompts a subsequent 2-electron reductive elimination of a diphosphonium cation [Ph$_3$PPPh$_3$]$^{2+}$, enabling formation of a transannular Sb–Sb bond to give [**4**]$^{4+}$. Analogous conversion of phosphine ligands into diphosphonium cations at electron-deficient phosphine metal complexes has been reported.[10] A space-filling view of the molecular structure of [**4**]$^{4+}$ (Figure S4) shows that limited space is available to accommodate two additional PPh$_3$ ligands and an optimization of the gas-phase geometry of **A$_1$** failed because of excessive steric stress between the phosphines.

Catenation of [(Ph$_3$P)Sb]$^+$ to give tetramer **B$_1$** and dimer **B$_2$** (Scheme 1), according to alternate route B, has precedent,

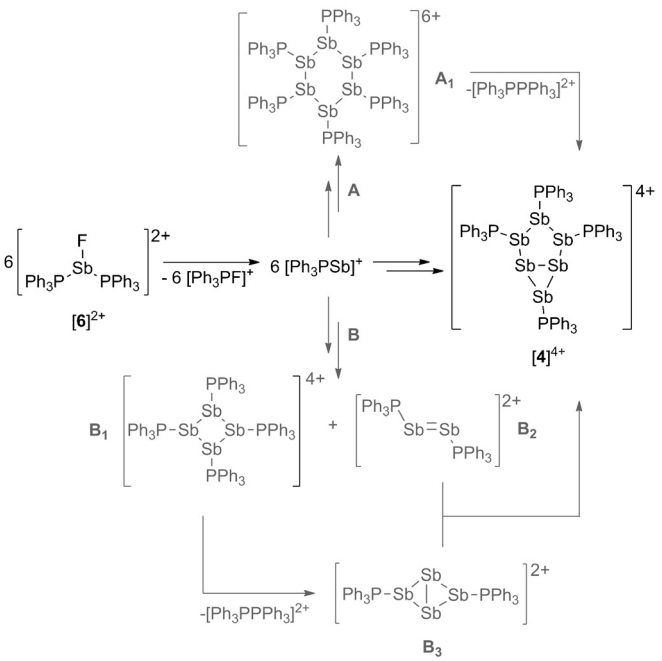

Scheme 1. Proposed steps in the reductive assembly of [**4**]$^{4+}$ from [**6**]$^{2+}$.

given the previous observation of [**1**]$^{2+}$ and [**2**]$^{4+}$.[4a–c] Subsequent reductive elimination of [Ph$_3$PPPh$_3$]$^{2+}$ from **B$_1$** would give the bicyclic dication **B$_3$**, a derivative of the previously reported [**3**]$^{2+}$, which is obtained through reductive catenation of PCl$_3$ and oxidation of AsPh$_3$ to [Ph$_3$AsAsPh$_3$]$^{2+}$.[4d] Elimination of [R$_3$PPR$_3$]$^{2+}$ was also detected upon heating derivatives of [**2**]$^{4+}$, with consequential precipitation of elemental antimony.[4c] Cycloaddition of intermediates **B$_2$** and **B$_3$** offers a plausible pathway to [**4**]$^{4+}$.

In summary, reaction mixtures of FSb(OTf)$_2$ and PPh$_3$ give the bisphosphine complex **6**(OTf)$_2$, which reductively eliminates [Ph$_3$PF][OTf] and undergoes catenation resulting in an overall 14-electron redox process, giving the triflate salt of a rare bicyclic polycation [**4**]$^{4+}$. This multi-electron reductive catenation features the simultaneous use of phosphines as ligands and reducing agents. Observation that interpnictogen complexes undergo discrete 2-electron, 8-electron, 18-electron, and now 14-electron redox catenation processes suggests the possibility of rationally targeting new intersections of structural and electronic complexity by a judicious choice of the redox active supporting ligand. The potential of exerting such control bodes well for achieving more extensively catenated pnictogen compounds, and for future structure–property studies of these intriguing *catena*-metal species.

Experimental Section

Standard inert atmosphere techniques were employed to handle reagents and solvents in an atmosphere of purified argon or nitrogen. See the Supporting Information for details.

[**4**][OTf]$_4$: FSb(OTf)$_2$ (5 mmol, 2.195 g) and PPh$_3$ (10 mmol, 2.620 g) were combined in MeCN (10 mL) in a thick-walled glass tube equipped with a magnetic stirrer. The tube was sealed and the

reaction mixture was stirred for 20 min at room temperature to give a clear yellow solution. The tube was then placed in an oil bath (90 °C) for 1.5 h to obtain a deep-red solution. The solution was filtered, concentrated to half its volume, layered with Et_2O (5 mL), and placed in the freezer at −30 °C for 72 h giving a fine orange powder. The supernatant was decanted and the powder was washed five times with MeCN (circa 3 mL) and dried under vacuum to give the product as a fine orange powder. Yield: 0.328 g, 17%. m.p. 114 °C (dec.); Elemental analysis (calcd/found; %): C (38.42/38.42) H (2.55/2.41) N (0.00/ < 0.3); IR (ATR, 298 K): $\tilde{\nu}$ = 220 (m), 248 (w), 311 (vw), 347 (w), 451 (m), 480 (s), 502 (vs), 514 (vs), 571 (m), 634 (s), 689 (s), 713 (m), 746 (m), 749 (m), 996 (s), 998 (m), 1024 (s), 1093 (m), 1151 (s), 1199 (m), 1235 (m), 1240 (s), 1268 (w), 1436 (w), 1480 (w) cm^{-1}; ^1H NMR (CD_3CN, 298 K, 300.3 MHz): δ = 7.01 (pseudo dd, 14 Hz, 8 Hz, 6 H), 7.38–7.51 (overlapping m, 18 H), 7.52–7.68 (overlapping m, 24 H), 7.68–7.80 ppm (overlapping m, 12 H); $^{13}C\{^1H\}$ NMR (CD_3CN, 298 K, 75.5 MHz): δ = 120.9 (q, $^1J_{CF}$ = 322 Hz), 120.6 (d, $^1J_{CP}$ = 58 Hz), 121.3 (d, $^1J_{CP}$ = 54 Hz), 122. 8 (d, $^1J_{CP}$ = 54 Hz), 130–131.3 (overlapping m), 133.3–135.5 ppm (overlapping m); $^{31}P\{^1H\}$ NMR (CD_3CN, 298 K, 121.5 MHz): δ = −3.2 (s, 1 P), −2.1 (s, 2 P), 7.62 ppm (broad s, 1 P); $^{19}F\{^1H\}$ NMR (CD_3CN, 298 K, 282.5 MHz): δ = −78.0 ppm (s). Needle-like crystals of [**4**][OTf]$_4$·2 MeCN·2 EtCN were obtained from a 1:1 MeCN:EtCN solution and exhibited the same ^{31}P NMR chemical shift as the bulk powder. Crystallographic details for [**4**][OTf]$_4$·2 MeCN·2 EtCN: formula = $C_{87}H_{78}F_{12}N_4O_{12}P_4S_4Sb_6$, M_w = 2582.15 g mol^{-1}, $P\bar{1}$, a = 13.3675(5), b = 16.4283(7), c = 23.2356(9) Å, α = 88.9560(10)°, β = 73.9250(10)°, γ = 81.9460(10)°, V = 4853.7(3) Å^3, T = 153.0 K, Z = 2, μ = 1.880, 76380 reflections measured, 28141 unique ($R_{int.}$ = 0.0243), R_1 = 0.0322, wR_2 = 0.0794 (all data).

6(OTf)$_2$: FSb(OTf)$_2$ (0.25 mmol, 0.109 g) and PPh_3 (0.50 mmol, 0.131 g) were combined in a flask as solids. While stirring rapidly, a minimum amount of MeCN (circa 1 mL) was added to dissolve the reagents. After complete dissolution, the pale yellow solution was stirred for a further 30 seconds and then the flask was placed under dynamic vacuum to rapidly evaporate the solvent, leaving a pale yellow powder. Yield: 0.237 g, 99%. m.p. 71–122 °C dec.; Elemental analysis: sample decomposes under vacuum, consistent with the high reactivity of this compound; IR (ATR, 298 K): $\tilde{\nu}$ = 222 (m), 228 (w), 318 (w), 354 (m), 394 (vw), 429 (m), 446 (m), 487 (vs), 512 (s), 529 (vw), 572 (m), 589 (m), 626 (vs), 688 (s), 708 (vw), 741 (s), 764 (vw), 801 (w), 835 (w), 849 (w), 951 (s), 983 (m), 997 (m), 1026 (w), 1070 (vw), 1093 (m), 1146 (s), 1184 (s), 1203 (s), 1227 (m), 1282 (w), 1347 (m), 1435 (m), 1480 (w), 1570 (w), 1646 cm^{-1} (w); ^1H NMR (CD_3CN, 298 K, 500.2 MHz): δ = 7.46 (broad pseudo t, 6 H), 7.50 (broad pseudo t, 6 H), 7.57 ppm (broad t, $^3J_{HH}$ = 6 Hz, 3 H); $^{13}C\{^1H\}$ NMR (CD_3CN, 298 K, 125.8 MHz): δ = 119.5 (q, $^1J_{CF}$ = 319 Hz), 129.2 (d, J_{CP} = 9 Hz), 131.2 (broad s), 134.1 ppm (d, J_{CP} = 14 Hz); $^{31}P\{^1H\}$ NMR (CD_3CN, 298 K, 202.5 MHz): δ = 16.0 ppm (broad s); $^{19}F\{^1H\}$ NMR (CD_3CN, 298 K, 282.5 MHz): δ = = −78.8 ppm (s). Crystals were obtained by cooling a saturated MeCN solution and exhibited the same ^{31}P NMR as the bulk powder. Crystallographic details for **6**(OTf)$_2$: formula = $C_{38}H_{30}F_7O_6P_2S_2Sb$, M_w = 963.43 g mol^{-1}, $P2_1/n$, a = 11.1964(4), b = 15.7917(6), c = 22.5109(8) Å, β = 94.9374(5)°, V = 3965.4(3) Å^3, T = 173 K, Z = 4, μ = 0.960, 36079 reflections measured, 9762 unique ($R_{int.}$ = 0.0239), R_1 = 0.0350, wR_2 = 0.0840 (all data).

CCDC-1057478 ([**4**][OTf]$_4$·2 MeCN·2 EtCN) and 1057479 (**6**-(OTf)$_2$) contains the supplementary crystallographic data for this paper. These data can be obtained free of charge from The Cambridge Crystallographic Data Centre via www.ccdc.cam.ac.uk/data_request/cif.

Keywords: antimony · catenation · phosphorus · reduction · structure elucidation

How to cite: *Angew. Chem. Int. Ed.* **2015**, *54*, 7828–7832
Angew. Chem. **2015**, *127*, 7939–7943

[1] a) N. Wiberg, *Coord. Chem. Rev.* **1997**, *163*, 217–252; b) G. Linti, H. Schnöckel, W. Uhl, N. Wiberg in *Molecular Clusters of the Main Group Elements* (Eds.: M. Driess, H. Nöth), Wiley-VCH, Weinheim, **2004**, pp. 126–168; c) N. Wiberg, P. P. Power in *Molecular Clusters of the Main Group Elements* (Eds.: M. Driess, H. Nöth), Wiley-VCH, Weinheim, **2004**, pp. 188–208; d) T. Chivers, I. Manners in *Inorganic Rings and Polymers of the p-Block Elements*, Royal Society of Chemistry, Cambridge, **2009**; e) S. Scharfe, F. Kraus, S. Stegmaier, A. Schier, T. F. Fässler, *Angew. Chem. Int. Ed.* **2011**, *50*, 3630–3670; *Angew. Chem.* **2011**, *123*, 3712–3754; f) T. F. Fässler, *Coord. Chem. Rev.* **2001**, *215*, 347–377; g) G. He, O. Shynkaruk, M. W. Lui, E. Rivard, *Chem. Rev.* **2014**, *114*, 7815–7880; h) M. Ruck, F. Locherer, *Coord. Chem. Rev.* **2015**, *285*, 1–10.

[2] For Se and Te, see: a) S. Brownridge, I. Krossing, J. Passmore, H. D. B. Jenkins, H. K. Roobottom, *Coord. Chem. Rev.* **2000**, *197*, 397–481; b) E. Ahmed, M. Ruck, *Coord. Chem. Rev.* **2011**, *255*, 2892–2903. For Si, see: c) S. Inoue, M. Ichinohe, T. Yamaguchi, A. Sekiguchi, *Organometallics* **2008**, *27*, 6056–6058; d) K. Takanashi, V. Y. Lee, T. Matsuno, M. Ichinohe, A. Sekiguchi, *J. Am. Chem. Soc.* **2005**, *127*, 9978–9979; e) A. Sekiguchi, T. Matsuno, M. Ichinohe, *J. Am. Chem. Soc.* **2000**, *122*, 11250–11251. For Ge, see: f) A. Sekiguchi, M. Tsukamoto, M. Ichinohe, *Science* **1997**, *275*, 60–61.

[3] a) R. D. Miller, J. Michl, *Chem. Rev.* **1989**, *89*, 1259–1410; b) H. Suzuki, S. Hoshino, K. Furukawa, K. Ebata, C. H. Yuan, I. Bleyl, *Polym. Adv. Technol.* **2000**, *11*, 460–467; c) T. Iwamoto, D. Tsushima, E. Kwon, S. Ishida, H. Isobe, *Angew. Chem. Int. Ed.* **2012**, *51*, 2340–2344; *Angew. Chem.* **2012**, *124*, 2390–2394; d) M. Kosa, M. Karni, Y. Apeloig, *Organometallics* **2007**, *26*, 2806–2814.

[4] a) E. Conrad, N. Burford, U. Werner-Zwanziger, R. McDonald, M. J. Ferguson, *Chem. Commun.* **2010**, *46*, 2465–2467; b) S. S. Chitnis, A. P. M. Robertson, N. Burford, J. J. Weigand, R. Fischer, *Chem. Sci.* **2015**, *6*, 2559–2574; c) S. S. Chitnis, Y. Carpenter, N. Burford, R. McDonald, M. J. Ferguson, *Angew. Chem. Int. Ed.* **2013**, *52*, 4863–4866; *Angew. Chem.* **2013**, *125*, 4963–4966; d) M. Donath, E. Conrad, P. Jerabek, G. Frenking, R. Fröhlich, N. Burford, J. J. Weigand, *Angew. Chem. Int. Ed.* **2012**, *51*, 2964–2967; *Angew. Chem.* **2012**, *124*, 3018–3021; e) M. Donath, M. Bodensteiner, J. J. Weigand, *Chem. Eur. J.* **2014**, *20*, 17306–17310.

[5] S. S. Chitnis, N. Burford, R. McDonald, M. J. Ferguson, *Inorg. Chem.* **2014**, *53*, 5359–5372.

[6] M. H. Holthausen, R. R. Hiranandani, D. W. Stephan, *Chem. Sci.* **2015**, *6*, 2016–2021.

[7] H. J. Breunig, K. H. Ebert, K. H. Gülec, J. Probst, *Chem. Ber.* **1995**, *128*, 599–603.

[8] a) G. Bellachioma, G. Cardaci, A. Macchioni, C. Venturi, C. Zuccaccia, *J. Organomet. Chem.* **2006**, *691*, 3881–3888; b) A. L. Filippou, E. O. Fischer, H. G. Alt, *J. Organomet. Chem.* **1988**, *344*, 215–225.

[9] a) T. Sasamori, Y. Arai, N. Takeda, R. Okazaki, N. Tokitoh, *Chem. Lett.* **2001**, 42–43; b) A. J. Roering, J. J. Davidson, S. N. MacMillan, J. M. Tanski, R. Waterman, *Dalton Trans.* **2008**, 4488–4498; c) R. Waterman, T. D. Tilley, *Angew. Chem. Int. Ed.* **2006**, *45*, 2926–2929; *Angew. Chem.* **2006**, *118*, 2992–2995.

[10] a) A. P. M. Robertson, N. Burford, R. McDonald, M. J. Ferguson, *Angew. Chem. Int. Ed.* **2014**, *53*, 3480–3483; *Angew. Chem.* **2014**, *126*, 3548–3551; b) A. P. M. Robertson, S. S. Chitnis, H. A. Jenkins, R. McDonald, M. J. Ferguson, N. Burford, *Chem. Eur. J.* **2015**, 21, 7902–7913; c) R. M. Siddique, J. M. Winfield, *Can. J. Chem.* **1989**, *67*, 1780–1784.

[11] a) A. Bondi, *J. Phys. Chem.* **1964**, *68*, 441 – 451; b) B. Cordero, V. Gómez, A. E. Platero-Prats, M. Revés, J. Echverria, E. Cremades, F. Barragán, S. Alvarez, *Dalton Trans.* **2008**, 2832 – 2838.

[12] The ^{31}P NMR spectrum of an equimolar mixture of PPh_3 and $FSb(OTf)_2$ initially shows only a singlet at $\delta = 28.5$ ppm, which is tentatively assigned to $[(Ph_3P)SbF(OTf)_2]$, analogous to the initial formation of **6**$(OTf)_2$ ($\delta = 16.0$ ppm) from a 2:1 mixture of PPh_3 and $FSb(OTf)_2$. Signals for $[Ph_3PF]^+$ and $[\mathbf{4}]^{4+}$ appear gradually upon stirring at room temperature for 5 days.

[13] A low temperature (−40 °C) ^{31}P NMR spectrum of an acetonitrile solution of **6**$(OTf)_2$ did not reveal any $^2J_{PF}$ coupling.

Received: April 3, 2015
Revised: May 7, 2015
Published online: June 3, 2015

